

## Polypropylene-organoclay nanocomposites containing nucleating agents

S. V. Ghugare · P. Govindaiah · C. V. Avadhani

Received: 13 May 2009 / Revised: 16 September 2009 / Accepted: 3 October 2009 /  
Published online: 17 October 2009  
© Springer-Verlag 2009

**Abstract** Polypropylene/organoclay nanocomposites containing nucleating agents, viz., aluminum hydroxybis[2,2-methylenebis(4,6-di-*tert*-butylphenyl) phosphate (NA21) and 1,3:2,4-bis(3,4-dimethylbenzylidene)sorbitol (Millad 3988), were prepared by direct melt intercalation in a twin-screw extruder. Nucleating agents were added to polypropylene during compounding and their effect on the properties of the nanocomposites was studied. X-ray diffraction (XRD) and transmission electron microscopy (TEM) exhibited clay layers to be intercalated and partially exfoliated. The expansion of inter-gallery distance of the clay layers was governed by the interaction between polypropylene, compatibilizer, and different nucleating agents. Thermogravimetric analysis (TGA) and differential scanning calorimetry (DSC) indicated higher thermal stability and crystallization temperature for nanocomposites compared to virgin polymer. Even a small addition of the nanoscale filler with 0.2% nucleating agents was found to promote concurrently several PP material properties, including improved tensile characteristics, higher Young's modulus, increased thermal stability and rate of crystallization.

**Keywords** Polypropylene nanocomposites · Organoclay · Nucleating agents · Thermogravimetric analysis · Transmission electron microscopy

### Introduction

The need for materials with superior mechanical, thermal, and processing properties cannot be over emphasized. Polymer–clay nanocomposites, a relatively new class of materials, show improved properties at very low loading levels compared with conventional filler composites [1]. This results in lighter materials with higher

---

S. V. Ghugare · P. Govindaiah · C. V. Avadhani (✉)

Polymer Science and Engineering Division, National Chemical Laboratory, Pune 411008, India  
e-mail: cv.avadhani@ncl.res.in

modulus and reduced linear thermal expansion making them desirable for several applications such as those that require high heat distortion temperature, higher stiffness, strength, and improved barrier properties [2]. Consequently, there is a pervasive use of polymer-nanocomposites in a gamut of applications, such as, automobile, electronics, and construction industries owing to their superior properties which are suitable replacements of metal parts in automotive applications [3, 4].

Polypropylene is one of the most interesting thermoplastic materials due to its low cost, low density, high heat distortion temperature, and extraordinary versatility in terms of properties and applications [5]. In order to improve polypropylene's competitiveness in engineering resin applications, it is desirable and important to increase dimensional stability, heat distortion temperature, stiffness, strength, barrier properties, and impact resistance without sacrificing the ease of processability.

The most commonly used clay is the smectite group mineral such as monmorillonite (MMT) [6]. Among the different methods of preparation of polymer/clay nanocomposites, the most versatile approach is based on direct polymer melt intercalation [7]. However, due to the low polarity of PP, it is difficult to obtain PP nanocomposite with homogeneous dispersion of the silicate layer at the nanometer level in the polymer. Organoclay containing silicate layers modified by nonpolar long alkyl groups are still relatively more polar and hence incompatible with polyolefin [8–12].

There are two widely used methods to prepare PP/clay nanocomposites (PPCN): (1) use of a polar functional oligomer as a compatibilizer [8–10]. In this approach, polyolefin oligomers with polar telechelic OH groups (PO–OH) and maleic anhydride-modified PP oligomers are used. The driving force for the intercalation is reckoned to originate from the strong hydrogen bonding between the OH groups of the PO–OH or maleic anhydride group or COOH group (generated from the hydrolysis of the maleic anhydride) and the oxygen groups of the silicates. The interlayer spacing of the clay increases and the interaction of the layers is weakened. The intercalated clay with the oligomers contacts PP under a strong shear field. If the miscibility of the oligomers with PP is good enough to disperse at the molecular level, exfoliation of the intercalated clay may occur [7]. (2) Clay is pre-dispersed in a polymer compatible with PP [13, 14]. In this method, organophilic clay is first dispersed in a solvent; unsaturated monomers are polymerized between the silicate layers in solvent environment and expand the interlayer spacing and form a polymer compatible with PP. After blending the polymer containing intercalated clay with PP, the silicate layers can be dispersed well in the PP matrix.

PP crystallizes slowly and results in reduced production yields. Addition of about 0.1–0.3% of nucleating agent induces the common  $\alpha$ -crystal modification of polymer and raises the peak crystallization temperature from about 110 °C to above 125 °C [15]. Therefore, it is interesting to study the effect of nucleating agents on compatibility, physical, and thermal properties of polypropylene nanocomposites.

The present study is, therefore, directed towards the use of commercially available nucleating agents (NA21 and Millad 3988) along with compatibilizer (PP-g-MA, Fusabond) and organo-modified clay (Cloisite 20A) to prepare PP-clay nanocomposites and to study the effect of nucleating agents on PP nanocomposites

with respect to thermal properties, crystallization behavior, morphology, and mechanical properties.

## Experimental

### Materials

Maleic anhydride-modified PP compatibilizer (PP-g-MA) (Fusabond M-613-05, DuPont) (**F**), organically modified clay (Cloisite 20A, Southern Clay Products) (**C**), and isotactic polypropylene, 2.9 MFI (Repol H029SG, Reliance Industries Ltd., Mumbai) were used as received. Polypropylene 12 MFI (reactor fluff—random ethylene-propylene copolymer with an ethylene content of about 3 mol %) (Reliance Industries Ltd., Mumbai) was stabilized with standard additive package prior to use. Commercial nucleating agents, viz., aluminum hydroxybis[2,2-methylenebis(4,6-di-*tert*-butylphenyl) phosphate (**NA21**) and 1,3:2,4-bis(3,4-dimethylbenzylidene)sorbitol (Millad 3988) (**M3988**) were used as received.

### Nanocomposite preparation

PP, compatibilizer, clay, and nucleating agents were thoroughly dispersed in acetone for 1 h and air dried first and then dried at 100 °C in a vacuum oven for 12 h to enable uniform coating of PP pellets with additives and filler. Berstorff twin-screw extruder (ZE25 with a mild mixing configuration) was used for the preparation of nanocomposites. The temperature of the extruder was maintained at 170, 175, 190, 200, 210, 215, 220, 225, and 230 °C from hopper to die, respectively. The screw speed was maintained at 100 and 50 rpm for PP (2.9 MFI) and PP (12 MFI), respectively. Extrudates from twin-screw extruder were pelletized on Haake pelletizer. Nanocomposite pellets were injection molded on DSM Micro-compounder to obtain tensile and Izod impact bars. Temperature of micro-compounder was maintained at 220 and 200 °C for 2.9 MFI and 12 MFI PP, respectively.

### Polymer characterization

#### *Thermogravimetric analysis (TGA)*

TGA-7 (Perkin-Elmer) was used to determine the thermal stability of the samples as well as the amount of clay present in the nanocomposites. The samples were heated under a draft of nitrogen from 50 to 600 °C at a heating rate of 10 °C/min, and the weight loss was recorded as a function of temperature.

#### *Differential scanning calorimetry (DSC)*

Thermal properties of the samples were analyzed on TA Instruments Q10 differential scanning calorimeter. Samples were heated in a draft of nitrogen from –50 to 200 °C at the rate of 10 °C/min and held for 1 min at the maximum

temperature. At the end of holding period the samples were cooled at the rate of 10 °C/min to record the crystallization exotherm.

### *XRD measurements*

Wide-angle X-ray diffractometer (WAXD) experiments were performed on Rigaku Dmax 2500 diffractometer equipped with a copper target and a diffracted beam monochromator (Cu K $\alpha$  radiation with  $\lambda = 1.5406 \text{ \AA}$ ) with a  $2\theta$  scan range of 20°–25° at room temperature. The nanocomposite specimens for WAXD were prepared by melt-pressing on Carver press at 180 °C.

### *Transmission electron microscopy (TEM)*

Samples for TEM were sectioned using a Lieca Ultracut UCT microtome. The sections were collected from water on 300 mesh carbon-coated copper grids. TEM imaging was carried out on JEOL 1200EX electron microscope operating at an accelerating voltage of 80 kV. Images were captured using a charged couple detector (CCD) camera for further analysis using Gatan Digital Micrograph analysis software.

### *Mechanical characterization*

Mechanical properties of the polypropylene nanocomposites under tensile test modes were tested on Instron 4204 universal testing machine, while the Notched Izod impact strength was measured on Ceast make impact tester.

## **Results and discussion**

Polypropylene nanocomposites were prepared by melt compounding method. Typically, PP (2.9 MFI and 12 MFI), PP-g-MA compatibilizer (F), organophilized clay (Cloisite 20A) (C) and nucleating agents (NA21 and Millad 3988) were compounded in a twin-screw extruder as shown in Table 1. PP-g-MA compatibilizer is known to improve interfacial adhesion between PP and fillers [4]. Different

**Table 1** Composition of various polypropylene nanocomposite samples

Sample code	Polypropylene (PP) 2.9/12 MFI			
	PP (%)	Compatibilizer (F) (%)	Clay 20A (C) (%)	Nucleating agent (%)
PP	100	–	–	–
PP-F	85	15	–	–
PP-M3988	100	–	–	0.2
PP-C	95	–	5	–
PP-F-C	80	15	5	–
PP-F-C-NA21	80	15	5	0.2
PP-F-C-M3988	80	15	5	0.2

nucleating agents were used in order to examine their effect on thermal properties, crystallization behavior, morphology development and mechanical properties.

### Thermal properties of PP nanocomposites

Clay content, as inorganic fraction, in PP nanocomposites, and their thermal stability ( $T_{10\%}$  and  $T_{50\%}$ ) were determined by TGA (Tables 2 and 3). TGA data for PP and PP nanocomposites show a single degradation step for all the samples.

PP nanocomposites prepared from 2.9 to 12 MFI resins indicated a marked increase in thermal stability compared to pure PP. The shift towards higher temperature may be attributed to the formation of a high-performance carbonaceous silicate char, that gets built up on the surface, insulating the underlying material and slowing the degradation and escape of volatile products generated during decomposition [16]. The shift may be also due to a chemical catalytic effect of the silicate as shown by Zanetti et al. [17]. The residue at high temperature (500 °C) is slightly higher for nanocomposites because of the higher inorganic content in filled materials (Tables 2 and 3).

However, thermal stability of PP nanocomposite with nucleating agents is not remarkably improved with respect to PP-C and PP-F-C indicating that thermal stability may only be improved marginally with added nucleating agents due to loss of semicrystalline morphology during degradation step. The very compact char layer formed that is responsible for the shift in weight loss curves, is not stable at high temperature and therefore it is degraded like the polymer matrix.

### Microstructure of PP nanocomposites

WAXD offers a convenient method to determine the interlayer spacing of the silicate layers in the original layered silicates and in the intercalated nanocomposites. However, only limited information about the spatial distribution of the silicate layers or any structural non-homogeneity in nanocomposites can be inferred. In WAXD patterns of nanocomposites, clay peak at about  $3.94^\circ$  shifts to lower angles with an increase in interlayer spacing ( $d$ -spacing = 2.47 nm) of clay galleries. In both grade PP (2.9 MFI and PP12 MFI) nanocomposites, there is an increase in interlayer  $d$ -spacing and gallery height (Table 4; Fig. 1A, B). The effect of nucleating agents on dispersion of clay 20A in PP matrix was investigated and the results indicated an increase in  $d$ -spacing in PP-F-C-NA21 and PP-F-C-M3988 as a function of the nucleating agent, being lower for NA21 (2.75 and 2.50 nm) and higher for Millad 3988 (3.0 and 2.9 nm) for PP 2.9 MFI and PP 12 MFI resin), respectively. Increased  $d$ -spacing indicates a wider separation of the silicate layers associated with polymer intercalation. XRD patterns indicate that the clay layers still maintained a relatively strong ordering of the resin layered structures in composites containing PP-C, PP-F-C, and NA21 indicating the clay layers to be intercalated and dispersed in PP matrix. However, Millad 3988-based composites exhibited relatively smaller peaks with a gradual increase in diffraction strength towards lower angles indicating the clay layers to be partially exfoliated and dispersed.

**Table 2** Thermal, physical and mechanical properties of nanocomposites based on polypropylene 2.9 MFI resin

Sample	Clay (wt%)	Melting point (°C)	Crystallization exotherm maximum (°C)	TGA		Young's modulus (MPa)	Tensile strength (MPa)	Notched Izod impact strength (kJ/m <sup>2</sup> )
				T <sub>10%</sub> (°C)	T <sub>50%</sub> (°C)			
PP	–	162	111	380	435	1,679 ± 36	33 ± 0.22	2.3
PP-F	–	163	116	420	465	1,808 ± 5	31 ± 1.36	1.5
PP-M3988	–	166	129	410	450	2,014 ± 15	35 ± 0.50	2.1
PP-C	1.8	165	116	425	435	1,843 ± 26	32 ± 0.86	2.1
PP-F-C	2.65	163	114	430	440	1,879 ± 10	30 ± 0.52	2.1
PP-F-C-NA21	2.74	164	121	435	445	1,965 ± 24	34 ± 0.85	1.5
PP-F-C-M3988	3.58	162	113	445	460	2,020 ± 29	35 ± 1	1.8

**Table 3** Thermal, physical and mechanical properties of nanocomposites based on polypropylene 12 MFI resin

Material	Clay (wt%)	Melting point (°C)	Crystallization exotherm maximum (°C)	TGA		Young's modulus (MPa)	Tensile strength (MPa)	Notched Izod impact strength (kJ/m <sup>2</sup> )
				T <sub>10%</sub> (°C)	T <sub>50%</sub> (°C)			
PP	–	144	101	420	460	1,121 ± 28	24 ± 0.75	3.1
PP-F	–	148	106	405	450	1,370 ± 18	24 ± 0.60	1.3
PP-M3988	–	145	119	410	450	1,184 ± 22	23 ± 0.34	1.6
PP-C	2.65	145	103	430	440	1,310 ± 20	25 ± 0.80	2.8
PP-F-C	3.50	148	107	450	460	1,686 ± 42	28 ± 1.2	2.1
PP-F-C-NA21	2.85	150	113	440	455	1,676 ± 40	31 ± 0.5	2.2
PP-F-C-M3988	3.60	148	108	445	460	1,949 ± 44	31 ± 0.22	2.6

**Table 4** Clay gallery height from WAXRD data of PP nanocomposites

Polypropylene (MFI)	<i>D</i> -spacing/clay gallery height (nm)			
	PP-C	PP-F-C	PP-F-C-NA21	PP-F-C-M3988
2.9	2.67/1.72	2.67/1.72	2.75/1.80	3.00/2.05
12	2.56/1.61	2.48/1.53	2.50/1.55	2.90/1.95

A range of nanocomposites with structures from intercalated to exfoliated can be obtained, depending on the degree of penetration of the polymer chains into the silicate galleries. So far, experimental results indicate that the outcome of polymer intercalation depends critically on silicate functionalization and constituent interactions. Vaia et al. [18] observed that an optimal interlayer structure on the organically modified layered silicate, with respect to the number per unit area and size of surfactant chains, is most favorable for nanocomposite formation, and intercalation depends on the existence of polar interaction between the organically modified layered silicate and the polymer matrix. Partial exfoliation was observed in PP nanocomposite with Millad 3988. This phenomenon may be attributed to the higher degree of interaction between the modified clay 20A and polar hydroxyl group of Millad 3988. Another possible explanation is that rapid nucleation and crystallization of PP inside the galleries of clay might push apart the clay layers causing larger *d*-spacing.

#### Crystal structure and crystallization behavior of PP nanocomposite

XRD patterns of PP and PP nanocomposites are shown in Fig. 2A, B. The XRD diffractograms indicate that there is no obvious difference between PP and PP nanocomposite in case of PP 12 MFI resin, but in the case of PP 2.9 MFI resin, the  $\beta$  phase of virgin PP ( $2\theta = 16.05$ ) disappears on compounding. The incipient  $\beta$  peak may disappear even for virgin PP merely by melt compounding. Addition of compatibilizer, clay, and nucleating agents does not affect the crystal structure of PP matrix in case of 12 MFI. It has been reported that addition of clay does not affect the crystal structure of the PP matrix [19].

Crystallization behavior of PP-nanocomposites was investigated by DSC. It was reported that clay 20A and compatibilizer (PP-MA) also nucleate PP [20]. The effect of nucleating agents on PP nanocomposites was investigated and it was observed that nucleating agents significantly enhanced the crystallization and melting temperature in PP nanocomposites without interfering with the crystal structure of PP matrix. In both grades of PP, addition of NA21 exhibited higher  $T_m$  and  $T_c$  compared to virgin PP and PP nanocomposites (Tables 2 and 3). However, in the case of PP nanocomposite containing Millad 3988,  $T_m$  and  $T_c$  were not significantly improved compared to nanocomposites containing clay and compatibilizer.

#### Transmission electron microscopy

Dispersibility of silicate layers in the composites was determined by TEM. The dark lines are the intersections of the silicate layers. In PP (2.9 MFI and 12 MFI)



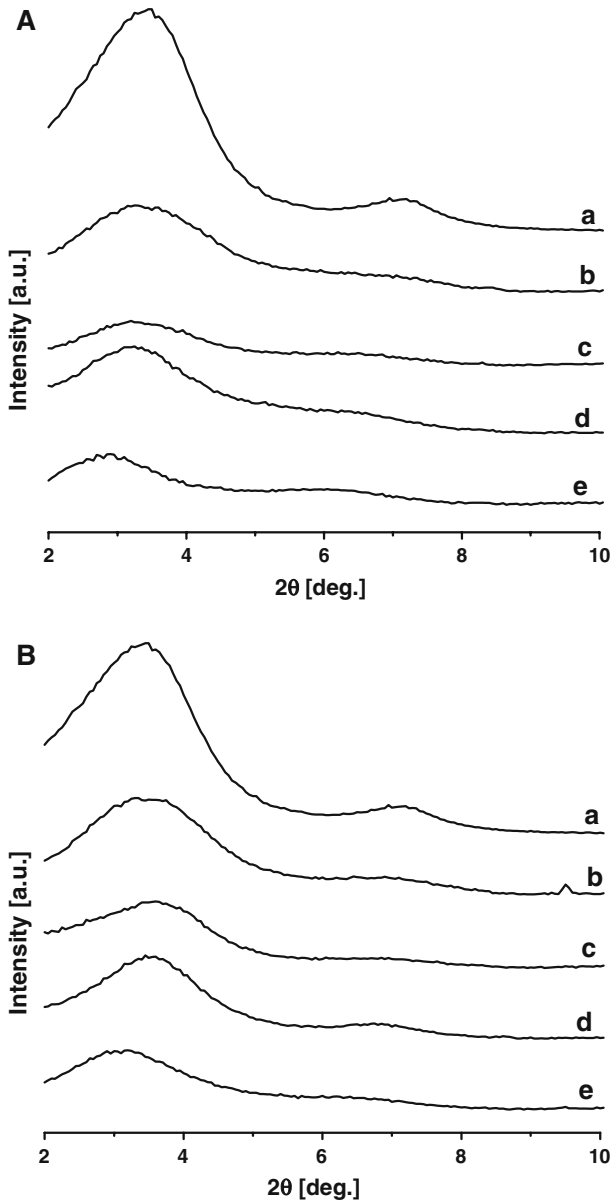


**Fig. 1** **A** WAXRD patterns of PP 2.9 MFI nanocomposite: (a) PP, (b) PP-C, (c) PP-F-C, (d) PP-F-C-NA21, (e) PP-F-C-M3988. **B** WAXRD patterns of PP 12 MFI nanocomposites: (a) PP, (b) PP-C, (c) PP-F-C, (d) PP-F-C-NA21, (e) PP-F-C-M3988

nanocomposites containing NA21 and Millad 3988, clay is dispersed homogeneously in the PP matrix as seen in Fig. 3A, B. From these micrographs it could be concluded that organophilized clay is well dispersed in PP matrix.

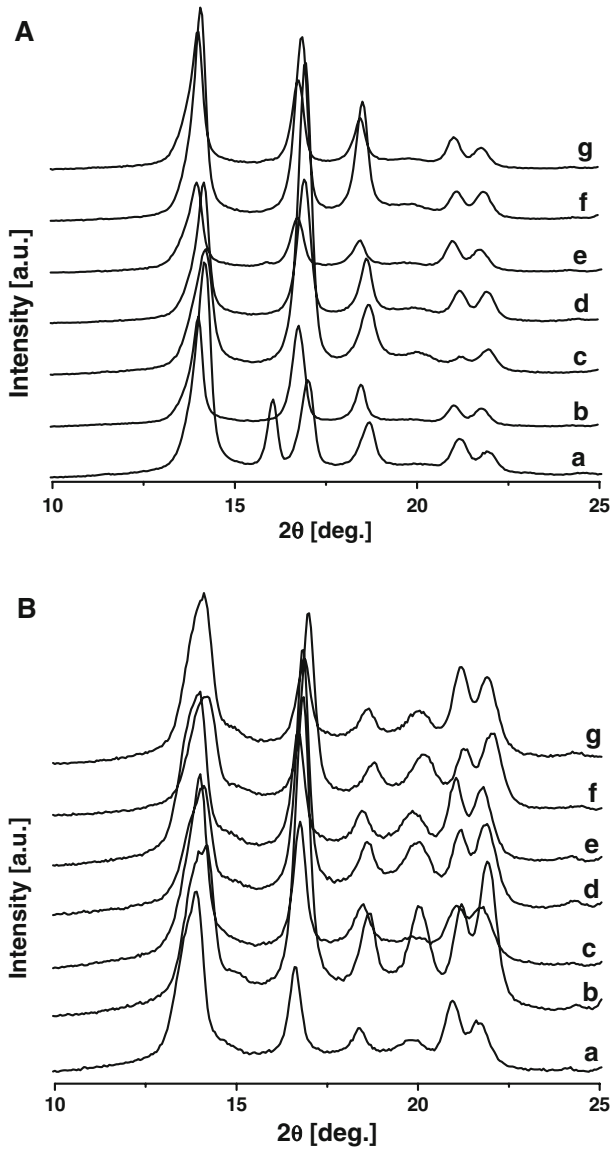


**Fig. 2** **A** WAXRD patterns of PP 2.9 MFI nanocomposite (a) PP, (b) PP-F, (c) PP-M3988, (d) PP-C, (e) PP-F-C, (f) PP-F-C-NA21, (g) PP-F-C-M3988. **B** WAXRD patterns of PP 12 MFI nanocomposite (a) PP, (b) PP-F, (c) PP-M3988, (d) PP-C, (e) PP-F-C, (f) PP-F-C-NA21, (g) PP-F-C-M3988

### Mechanical properties of PP nanocomposites

Young's modulus, tensile strength, and notched Izod impact strength were measured on tensile and Izod impact bars. Young's modulus and tensile strength increased upon addition of compatibilizer and clay, which further increased upon addition of

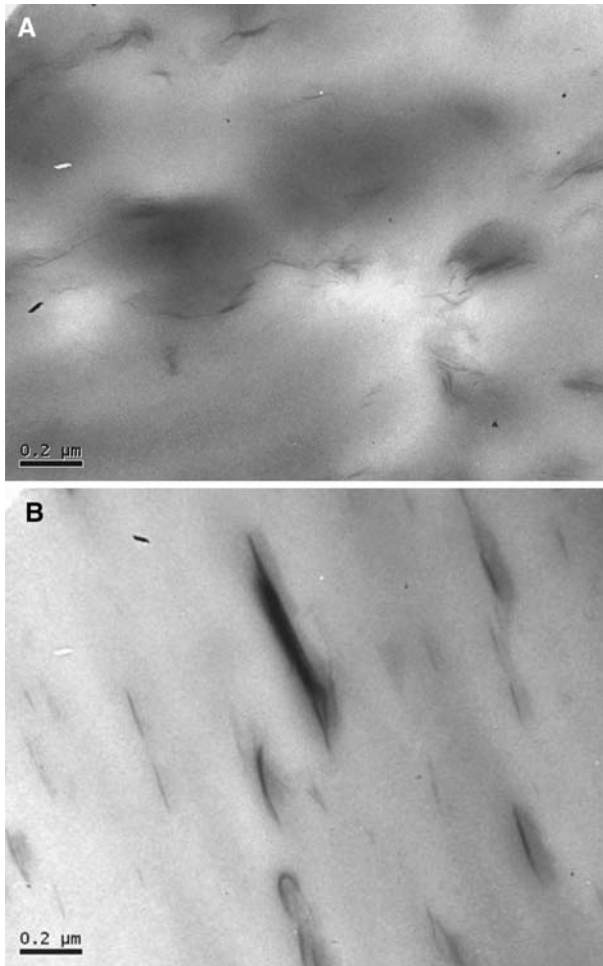


**Fig. 3** **A** TEM image of PP (2.9 MFI)-F-C-NA21 nanocomposite. **B** TEM image of PP (12 MFI)-F-C-NA21 nanocomposite

nucleating agents (Tables 2 and 3; Fig. 4A, B). Of primary importance among the mechanical properties of composites is tensile stress at the yield point. Filler dispersion and adhesion with the polymer matrix are of great importance for improving the mechanical behavior of composites. Fine control of the interface morphology of the polymer nanocomposites is one of the most critical parameter to impart desired mechanical properties of such materials. This depends mainly on the microstructure, including the interfacial bonding as well as the form and size distribution of the filler, its spatial distribution on the matrix, the thickness of the interface, etc. When there is a poor binding between the matrix and the filler, the composite is brittle because the applied load may not be transferred to the filler [21].

However, the nanocomposites exhibited poor impact resistance probably due to maleic anhydride grafting process that may be accompanied by chain scission [22].

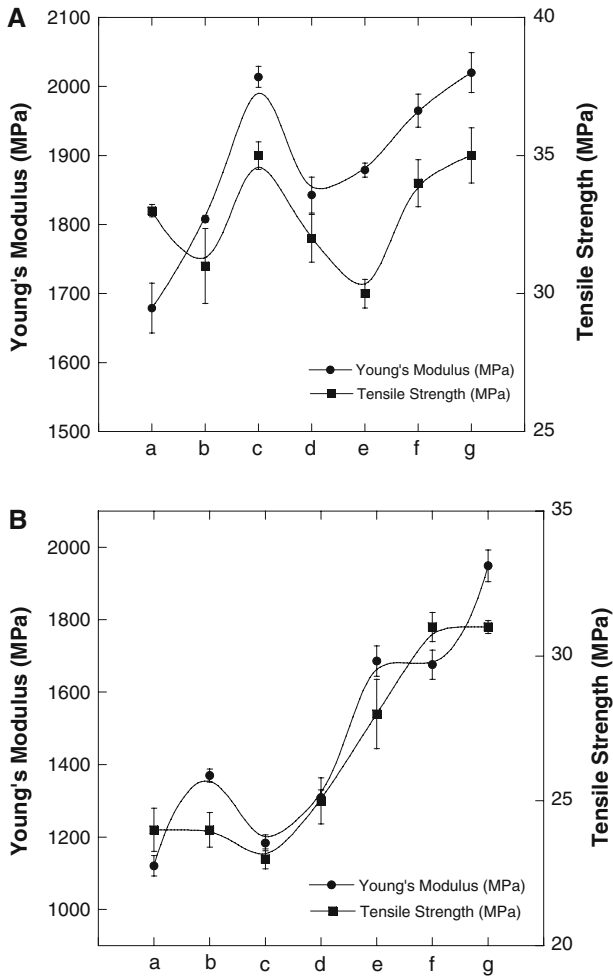


**Fig. 4** **A** Mechanical properties of PP (2.9 MFI) nanocomposite (a) PP, (b) PP-F, (c) PP-M3988, (d) PP-C, (e) PP-F-C, (f) PP-F-C-NA21, (g) PP-F-C-M3988. **B** Mechanical properties of PP (12 MFI) nanocomposite (a) PP, (b) PP-F, (c) PP-M3988, (d) PP-C, (e) PP-F-C, (f) PP-F-C-NA21, (g) PP-F-C-M3988

## Conclusion

PP-organophilized clay nanocomposites were successfully prepared by melt mixing of PP with PP-g-MA and different nucleating agents (NA21 and Millad 3988). XRD and TEM indicate the formation of composites in which the clay particles were well dispersed and partial exfoliation of silicate layers was observed in composites containing Millad 3988. Upon formation of PP nanocomposites,  $T_m$  and  $T_c$  increased which increased further upon addition of nucleating agents. Mechanical properties of PP nanocomposites containing nucleating agents showed significant

improvement in Young's modulus and tensile strength when compared to neat PP, PP/clay, and PP/PP-g-MA/clay composition.

## References

1. Garcés JM, Moll DJ, Bicerano J, Fibiger R, McLeod DG (2000) Polymeric nanocomposites for automotive applications. *Adv Mater* 12:1835–1839
2. Reichert P, Nitz H, Klinkle S, Brandsch R, Thomann R, Mulhaupt R (2000) Poly(propylene)/organoclay nanocomposite formation: influence of compatibilizer functionality and organoclay modification. *Macromol Mater Eng* 275:8–17
3. Usuki A, Kojima Y, Kawasumi M, Okada A, Fukushima Y, Kurauchi T, Kamigaito O (1993) Synthesis of nylon 6-clay hybrid. *J Mater Res* 8:1179–1184
4. Kojima Y, Usuki A, Kawasumi M, Okada A, Fukushima Y, Kurauchi T, Kamigaito O (1993) Mechanical properties of nylon 6-clay hybrid. *J Mater Res* 8:1185–1189
5. Moore EP Jr (1996) Polypropylene handbook. Hanser Publishers, New York
6. Whittingham MS, Jacobson AJ (1982) Intercalation chemistry. Academic Press, New York
7. Sinha Ray S, Okamoto M (2003) Polymer/layered silicate nanocomposites: a review from preparation to processing. *Prog Polym Sci* 28:1539–1641
8. Kawasumi M, Hasegawa N, Kato M, Usuki A, Okada A (1997) Preparation and mechanical properties of polypropylene-clay hybrids. *Macromolecules* 30:6333–6338
9. Hasegawa N, Kawasumi M, Kato M, Usuki A, Okada A (1998) Preparation and mechanical properties of polypropylene-clay hybrids using a maleic anhydride-modified polypropylene oligomer. *J Appl Polym Sci* 67:87–92
10. Kato M, Usuki A, Okada A (1997) Synthesis of polypropylene oligomer—clay intercalation compounds. *J Appl Polym Sci* 66:1781–1785
11. Giannelis EP (1996) Polymer layered silicate nanocomposites. *Adv Mater* 8:29–35
12. Morgan AB, Harris JD (2003) Effects of organoclay soxhlet extraction on mechanical properties, flammability properties and organoclay dispersion of polypropylene nanocomposites. *Polymer* 44:2313–2320
13. Kurokawa Y, Yasuda H, Kashiwagi M, Oyo A (1997) Structure and properties of a montmorillonite/polypropylene nanocomposite. *J Mater Sci Lett* 16:1670–1672
14. Kurokawa K, Yasuda H, Oyo A (1996) Preparation of nanocomposites of polypropylene and smectite. *J Mater Sci Lett* 15:1481–1483
15. Blomenhofer M, Ganzleben S, Hanft D, Schmidt H-W, Kristiansen M, Smith P, Stoll K, Maeder D, Hoffmann K (2005) “Designer” nucleating agents for polypropylene. *Macromolecules* 38:3688–3695
16. Alexandre M, Dubois P (2000) Polymer-layered silicate nanocomposites: preparation, properties and uses of a new class of materials. *Mater Sci Eng* 28:1–63
17. Zanetti M, Camino G, Reichert P, Mulhaupt R (2001) Thermal behaviour of poly(propylene) layered silicate nanocomposites. *Macromol Rapid Commun* 22:176–180
18. Vaia RA, Giannelis EP (1997) Polymer melt intercalation in organically-modified layered silicates: model predictions and experiment. *Macromolecules* 30:8000–8009
19. Liu X, Wu Q (2001) PP/clay nanocomposites prepared by grafting-melt intercalation. *Polymer* 42:10013–10019
20. Chiu FC, Lai SM, Chen JW, Chu PH (2004) Combined effects of clay modifications and compatibilizers on the formation and physical properties of melt-mixed polypropylene/clay nanocomposites. *J Polym Sci B* 42:4139–4150
21. Bikiaris DN, Vassiliou A, Pavlidou E, Karayannidis GP (2005) Compatibilization of PP-g-MA copolymer on iPP/SiO<sub>2</sub> nanocomposites prepared by melt mixing. *Eur Polym J* 41:1965–1978
22. Garcio-Lopez D, Picazo O, Merino JC, Pastor JM (2003) Polypropylene-clay nanocomposites: effect of compatibilizing agents on clay dispersion. *Eur Polym J* 39:945–950